DYNAMIC ANALYSIS OF JACK-UP UNITS IN SOFT CLAY OVERLYING SAND

Yifa Wang* and Mark J. Cassidy
Department of Infrastructure Engineering, Faculty of Engineering and Information Technology
THE UNIVERSITY OF MELBOURNE

* *corresponding author: yifa.wang@unimelb.edu.au*

ABSTRACT
Jack-up vessels, with their heavy crane capacity, are pivotal in offshore wind turbine installation and maintenance. Accurate site-specific assessment is vital for their safe operation amidst challenging layered seabed and storm loads. Due to their flexibility, the dynamic response of jack-up units hinges on nonlinear foundation behaviour. Precise foundation stiffness modelling reduces critical member stress and refines natural frequency, enhancing dynamic attributes. A recent macro-element model, that accounts for the force resultant behaviour of the inverted conical spudcan footing and is tailored to clay overlying sand conditions, has been integrated into structural analysis to evaluate the jack-up's pushover capacity. Significant soil layer effects observed during static loading are anticipated to persist under dynamic loading conditions. This study analyses nonlinear jack-up dynamics under storm loading, employing the macro-element foundation model and NewWave theory for wave loading. Example analyses highlight how a strong sand layer beneath clay influences dynamic jack-up response. The results provide insights into the understanding of offshore platforms in a layered seabed.

KEY WORDS: jack-up; spudcan foundations; macro-element modelling; fluid-structure-soil interaction; NewWave; clay overlying sand

INTRODUCTION

Jack-up units play a pivotal role in offshore oil and gas (O&G) drilling operations within shallow to moderate water depths. As the offshore wind energy sector flourishes, jack-up vessels have gained prominence in facilitating the installation and maintenance tasks associated with offshore wind turbines. A jack-up vessel, characterised as a self-elevating barge, possesses the capability to elevate its hull above the ocean's surface, thereby establishing a stable platform for heavy lifting operations. By relying on three retractable legs firmly sitting on the ocean floor, each linked to a spudcan foundation, jack-up units secure their stability. In offshore wind construction, four or six legs are becoming more common. Spudcans, defined as saucer-shaped polygonal, or quasi-circular foundations with a central spigot and a gently sloping conical underside, play a crucial role in determining the interaction between jack-up units and seabed soils. The typical diameter of these spudcans ranges from 6-14 m for offshore wind installation jack-up vessels and extends to 10-20 m for O&G jack-up rigs.

The intricate response of jack-up units, being slender and dynamic sensitive structures, to environmental forces hinges upon the interaction between spudcans and the underlying seabed soils. During a storm event, large lateral forces induced by wind, waves, and current subject the spudcan foundations to combined vertical (V), horizontal (H), and moment (M) reaction forces. Simplifying the intricate foundation behaviours under such complex loading combinations by treating them to pinned joints or linear spring sets tends to overlook the non-linear geotechnical behaviour and does not allow prediction of jack-up failures involving, for example, shallow sliding of a windward spudcan or plunging of leeward spudcan noted in physical tests. Furthermore, these models fail to emulate the evolving foundation stiffness that unfolds during operational phases.

In response to these challenges, several macro-element models have been devised based on the principles of strain-hardening plasticity theory. The appeal of macro-element models lies in encapsulating non-linear soil-structure interactions within distinct macro-elements, articulated through force resultants acting on the foundation and their conjugate displacements. This terminology is consistent with that used in structural engineering, and the model can be seamlessly integrated into numerical structural analyses. While existing macro-element models addressing spudcan behaviour include those proposed by Schotman (1989)[1]; Dean et al. (1997a[2], 1997b[3]); van Langen et al. (1999)[4]; Martin and Houlsby (2001)[5]; Cassidy et al. (2002)[6]; Houlsby and Cassidy (2002)[7]; Bienen et al. (2006)[8]; Vlahos et al. (2006)[9]; Zhang et al. (2014)[10]; Cheng and

Cassidy (2016)[11], encompassing a range of soil types and loading scenarios, they remain confined to single-layer soils.

This paper investigates behaviour in seabeds of clay overlaying sand. During the process of installing and preloading jack-up units in clay overlying sand, a squeezing mechanism is mobilised, characterised by a significant increase in vertical bearing capacity (for the same depth, when compared to the pure clay seabed). This squeezing stands apart from the two conventional soil failure mechanisms observed in pure clay, namely, general shear failure in stiff clay and deep failure in soft clay, as shown in Figure 1. Two macro-element models, introduced by Martin and Houlsby (2001)[5] and Zhang et al. (2014)[10], cater to these distinct scenarios. Martin and Houlsby (2001)[5]'s model, labelled as Model B, was developed from a series of 1*g* model tests conducted on heavily overconsolidated clay, revealing an open cavity due to the high ratio of clay strength to the overburden pressure. In contrast, Zhang et al. (2014)[10]'s model drew upon centrifuge model tests performed on normally consolidated clay, incorporating a substantial soil backflow that envelops the upper portion of the spudcan.

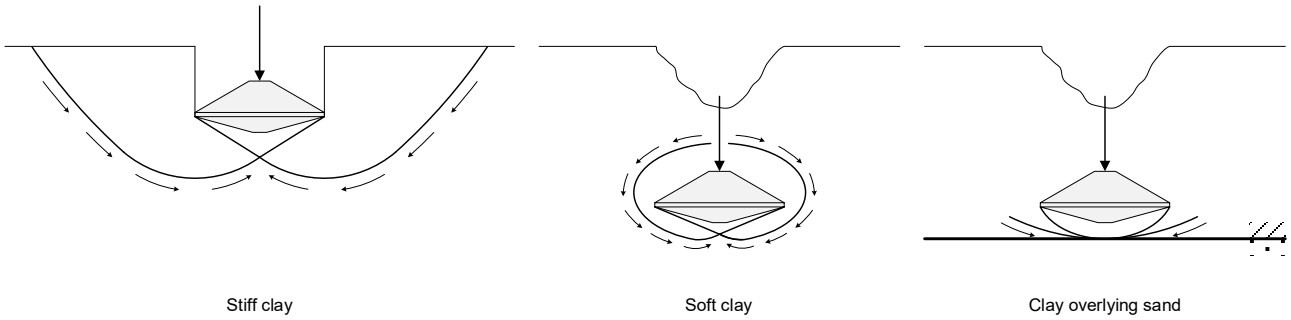

Figure 1. Spudcan bearing failure mechanisms in clay and clay overlying sand

Recognising the pivotal role of the underlying sand layer in shaping the combined loading capacity of the spudcan, Wang et al. (2023)[12] introduced a macro-element model tailored to clay overlying sand conditions. This model was integrated within the jack-up structural analysis, facilitating quasi-static pushover analyses (Wang et al., 2022[13]). The soil layering is found to significantly influence the overall jack-up response under static loading conditions. Wang et al. (2022)[13] simplified the wind, wave and current-induced forces to single-point pushover loads on the structure. However, a more realistic modelling approach to environmental loading could potentially yield greater insights into the dynamic behaviour of these slender structures. This assumption proves pivotal, as the precision in modelling foundation stiffness serves to reduce critical member stress and the natural frequency of the structure, thereby refining the dynamic attributes of the jack-up unit as it navigates away from the dominant wave period prevalent in the ocean.

In this paper, nonlinear dynamic analyses on jack-up units subjected to storm loading are conducted. The macro-element model formulated for clay overlying sand is used for the foundation model, while the spectral content of wave loading is considered using NewWave theory. A comprehensive comparison of macro-element models for pure clay and clay-over-sand conditions is presented. Example dynamic analyses shed light on the profound influence of the underlying strong sand layer on the dynamic response of jack-up structures.

FLUID-STRUCTURE-SOIL INTERACTION MODELLING

The dynamic analyses were carried out using the structural analysis program SOS_3D, developed by Bienen and Cassidy (2006)[14]. This paper outlines the principal characteristics of the structural, foundation, and wave modelling models utilised in SOS_3D, however, additional information can be referenced from Bienen and Cassidy (2006)[14]. The numerical analyses adhere to common field practice procedures. The initial step involves installing the jack-up, by vertical preloading to twice its self-weight. This is accomplished by applying point loads to the leg-hull connections. This procedure serves as a proof test for the spudcans, subjecting the foundations to a greater vertical load than anticipated during regular operation. Following the preloading phase, the jack-up's weight is adjusted to its self-weight, simulating the discharge of ballast water. Subsequently, the wave loading is applied to the jack-up.

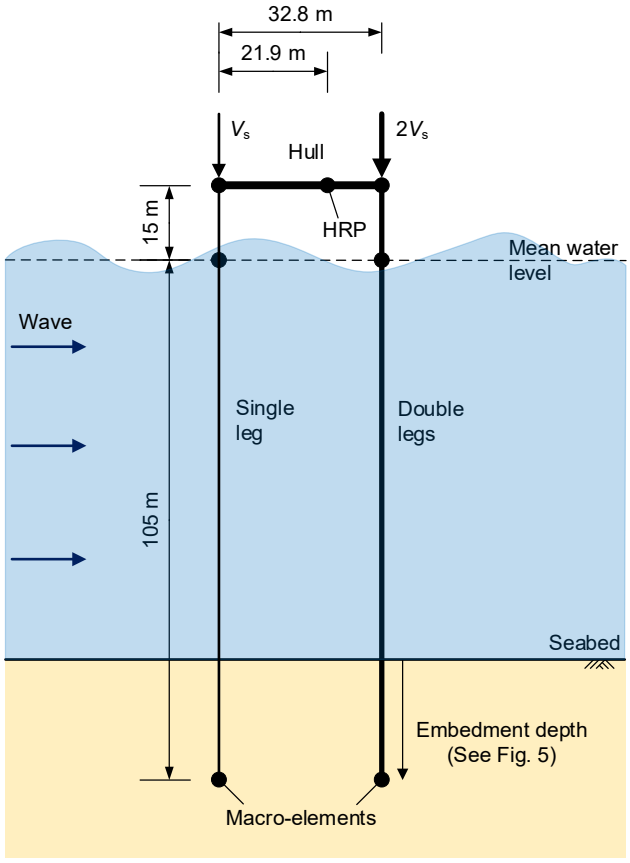

Figure 2. The jack-up structural model used in dynamic analyses

Table 1. Properties of the jack-up unit and soil used in the analyses

Jack-up and spudcan properties			
Leg length	120 m	Water hull clearance	15 m
Transverse leg spacing	43.28 m	Longitudinal leg spacing	39.32 m
Young's modulus, E	200 GPa	Shear modulus, G	80 GPa
Equivalent area, A_{leg}	0.58 m^2	Equivalent area, A_{hull}	2.0 m^2
Second moment of area, I_{leg}	10.843 m^4	Second moment of area, I_{hull}	40 m^4
Shear area, $A_{s,\,leg}$	0.04 m^2	Shear area, $A_{s,\,hull}$	0.2 m^2
Hydraulic area, $A_{h,\,leg}$	3.94 m^2	Hydraulic area, $A_{h,\,hull}$	3.94 m^2
$Mass_{leg}$	2.0E6 kg	$Mass_{hull}$	16.1E6 kg
Spudcan diameter, D	14 m		
Clay properties			
The depth of the clay layer, H_c	21 m	Submerged unit weight, γ_c'	6.85 kN/m^3
Shear strength at the mudline, s_{um}	1.0 kPa	Shear strength gradient, k	1.5 kPa/m
Sensitivity, S_t	2.0	Ductility, ξ_{95}	30
Rigidity index, $I_r = G_{clay}/s_u$	100		
Sand properties			
Submerged unit weight, γ_s'	10.0 kN/m^3	Shear modulus ratio, G_{sand}/G_{clay}	10
Friction angle, ϕ	33°	Footing roughness, α	0.5

STRUCTURAL MODELLING

The schematic diagram in Figure 2 illustrates the basic two-dimensional plane frame model used to analyse the three-legged jack-up unit. Environmental forces are assumed to act along the jack-up's axis of symmetry, with one leg windward and two legs leeward. The jack-up's hull and legs are modelled by equivalent beam elements, with the corresponding stiffnesses and masses given in Table 1. Rigid leg-hull connections are assumed, as accurately modelling the intricate leg jacking and locking mechanisms is complex. *P*-Δ effects, axial load, and shear effects are incorporated in SOS_3D and the unconditionally stable Newmark $\beta = 1/4$ method is chosen for solving the dynamic equations. Structural damping is set at 5% for the low surge and sway modes.

FOUNDATION MODELLING

The spudcan foundations are depicted using the macro-element model proposed by Wang et al. (2023)[12]. Each foundation is connected to the appropriate structural node, as shown in Figure 2. This macro-element model was specifically designed to represent the behaviour of spudcan foundations in clay overlying sand seabed soils.

The model itself is underpinned by the strain-hardening plasticity theory and encompasses four essential components: (a) a yield surface delineating the boundary between elastic and plastic states within the combined *VHM* load space; (b) a hardening law governing how the size of the yield surface evolves with vertical plastic displacement; (c) a matrix that captures the elastic behaviour for any load increments within the yield surface; (d) a flow rule that defines the ratios between the plastic displacement components of the footing during yield.

Figure 3 shows the vertical, horizontal, and rotational degrees of freedom for a typical spudcan footing. Upon preloading the spudcan to a specified vertical load magnitude V_0, a yield surface is established with its dimensions defined by V_0. When the load changes within this yield surface, the response remains elastic. However, the elasto-plastic behaviour becomes evident when the load state reaches the boundaries of the yield surface. Subsequent plastic penetration of the spudcan triggers the expansion of the yield surface, altering its shape as it approaches the underlying sand layer, as shown in Figure 4.

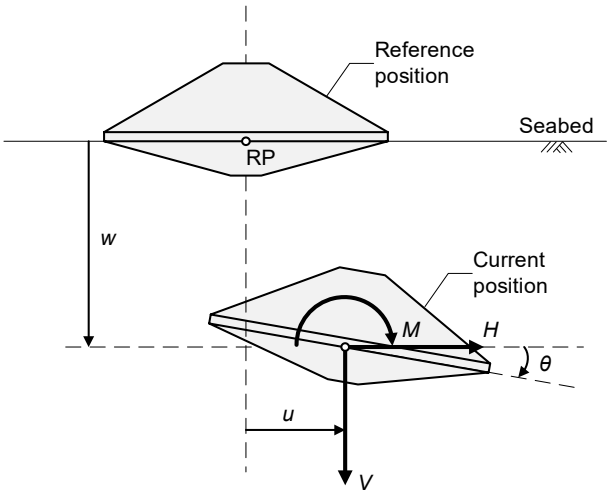

Figure 3. Combined loads on a spudcan footing

Table 2 summarises the recommended formulations for the macro-element models applicable to spudcan foundations in both pure clay and clay-over-sand conditions, as presented by Martin and Houlsby (2001)[5], Zhang et al. (2014)[10], Wang et al. (2023)[12]. Notably, the table highlights differences in aspects such as the hardening law, the shape of the yield surface, coefficients related to elasticity, and the flow rule. It also indicates the interrelationships between these formulations.

Table 2. Macro-element models developed for clay and clay overlying sand

Model component	Constant	Explanation	Main equation	Pure clay Model B	Pure clay Zhang et al. (2014)[10]'s model	Clay-over-sand Wang et al. (2023)[12]'s model
Hardening law				General shear failure without backflow, see Houlsby and Martin (2003)[18]	Incorporates deep failure with backflow, see Hossain and Randolph (2009)[19]	Squeezing failure, see Wang et al. (2021)[20]
Yield surface	h_0	Dimension of yield surface	$f=\left(\frac{H}{h_0V_0}\right)^2+\left(\frac{M/D}{m_0V_0}\right)^2-\frac{2eHM/D}{h_0m_0V_0^2}$ $-\left[\frac{(\beta_1+\beta_2)^{(\beta_1+\beta_2)}}{\beta_1^{\beta_1}\beta_2^{\beta_2}}\cdot\frac{1}{(1+\chi)^{(\beta_1+\beta_2)}}\right]^2$ $\times\left(\frac{V}{V_0}+\chi\right)^{2\beta_1}\left(1-\frac{V}{V_0}\right)^{2\beta_2}=0$	0.127	Vary with depth and clay sensitivity, see Zhang et al. (2014)[21]	Scaled from pure clay parameters, see Wang et al. (2020)[22] for the scaling factors
	m_0	Dimension of yield surface		0.083		
	E	Eccentricity of yield surface		Vary with vertical load, see Martin and Houlsby (2001)[5]		
	X	Ratio of tensile to compressive capacity		0	0.6	Vary with depth, see Wang et al. (2022)[13]
	β_1	Curvature factor for yield surface (low stress)		0.764	1.0	0.37
	β_2	Curvature factor for yield surface (high stress)		0.882	1.0	0.87
Elastic behaviour	G_{clay}	Shear modulus of clay	$\begin{bmatrix}\delta V\\ \delta H\\ \delta M/D\end{bmatrix}=\frac{G_{clay}D}{8}\begin{bmatrix}4K_v & 0 & 0\\ 0 & 4K_h & 2K_c\\ 0 & 2K_c & K_m\end{bmatrix}\begin{bmatrix}\delta w_e\\ \delta u_e\\ D\delta\theta_e\end{bmatrix}$	$G_{clay}=I_r s_u$, see Cassidy et al. (2002)[23] for selection of I_r		
	K_v, K_h, K_m, K_c	Elastic stiffness coefficients		see Doherty and Deeks (2003)[24]	see Zhang et al. (2012)[25]	see Wang et al. (2020)[26]
Flow rule	Z	Non-association parameter	$\partial w_p=\zeta\partial w_{p,\,associated}$	0.6	—	—
	α_v	Association parameter (vertical)		—	1.1	1.1

	α_h	Association parameter (horizontal)	$g=\left(\frac{H}{\alpha_h h_0 V_0^{'}}\right)^2+\left(\frac{M/D}{\alpha_m m_0 V_0^{'}}\right)^2-\frac{2eHM/D}{\alpha_h\alpha_m h_0 m_0 V_0^{'2}}$ $-\alpha_v^2\left[\frac{(\beta_3+\beta_4)^{(\beta_3+\beta_4)}}{\beta_3^{\beta_3}\beta_4^{\beta_4}}\cdot\frac{1}{(1+\chi)^{(\beta_3+\beta_4)}}\right]^2$ $\times\left(\frac{V}{V_0^{'}}+\chi\right)^{2\beta_3}\left(1-\frac{V}{V_0^{'}}\right)^{2\beta_4}=0$	—	1.0	1.0
	α_m	Association parameter (moment)		—	1.35	1.0
	β_3	Modified curvature parameter (low stress)		—	0.45	0.20
	β_4	Modified curvature parameter (high stress)		—	0.45	0.45

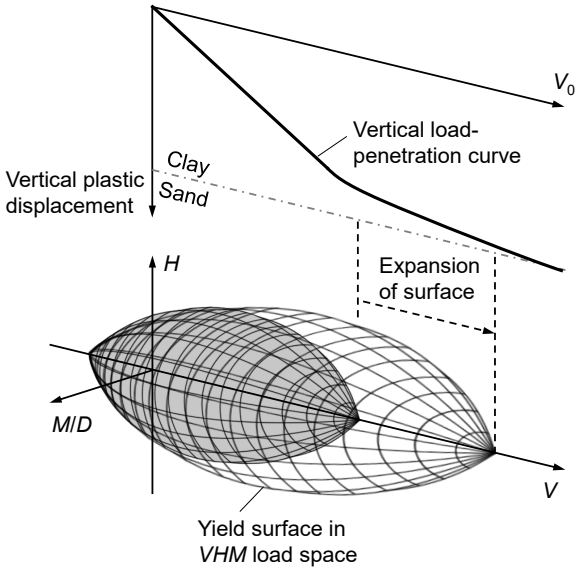

Figure 4. Expansion of yield surface with spudcan penetration

WAVE MODELLING

The NewWave theory, as outlined by Tromans et al. (1991)[15], is employed in evaluating surface elevations and wave kinematics within SOS_3D. NewWave accommodates the spectral composition of the sea state while retaining deterministic characteristics (Taylor et al., 1997[16]; Cassidy et al., 2001[17]). Pierson-Moskowitz wave spectrum is used to represent the NewWave shape, with a significant wave height H_s = 12 m and a mean-crossing period T_z = 10.65 s. For determining wave kinematics near the crest, delta stretching is used. The fluid drag C_d and inertia C_m coefficients are set at 1.1 and 2.0, respectively. The crest of the NewWave is located in horizontal space at the hull reference point at time t = 0 s (HRP in Figure 2). Its vertical elevation is below the hull at the amplitude specified in the analysis (a = 8, 12 and 15 m).

The hydrodynamic forces on the jack-up legs are computed using the extended Morison equation that considers relative motions. This equation incorporates added mass and hydrodynamic matrices. Equivalent nodal loads are calculated by integrating distributed loading using 7-point Gaussian integration and the appropriate shape function. This analysis focuses solely on the impact of pure wave loading, excluding any consideration of current or wind effects.

DYNAMIC ANALYSES

EXAMPLE RESULTS

The load-displacement curve illustrating the spudcan preloading within a clay layer overlying sand is presented in Figure 5, accompanied by a comparative analysis with results from the pure clay scenario. The soil properties can be found in Table 1, focusing on a normally consolidated clay layer overlying a medium-dense sand layer. The bearing capacity in the pure clay condition exhibits a linear increase trend, corresponding to the progressive enhancement of soil strength with increasing depth, and the slight increase in the bearing capacity factors. Notably, as the spudcan approaches the underlying sand layer, there is a significant increase in vertical bearing pressure. This divergence from the behaviour observed in the pure clay becomes apparent at a depth of 0.4D above the clay-sand interface. Between this depth and the sand surface is defined as the influence zone, a region wherein the spudcan is capable of detecting the presence of the strong underlying sand layer. Moreover, the failure mechanism within this influence zone can be characterised as a squeezing failure.

To examine the dynamic aspects, analyses have been conducted at four spudcan embedments, each falling within the confines of the influence zone (referred to as DYN1 through DYN4 in Figure 5). Among these, DYN2 (characterised by a representative preload of 400 kPa) has been selected as the baseline reference. Comparative investigations with dynamic analyses in the pure clay condition have been undertaken at both DYN5 and DYN6. These instances correspond respectively to the same embedment depth and preload magnitude as observed in the clay-over-sand condition.

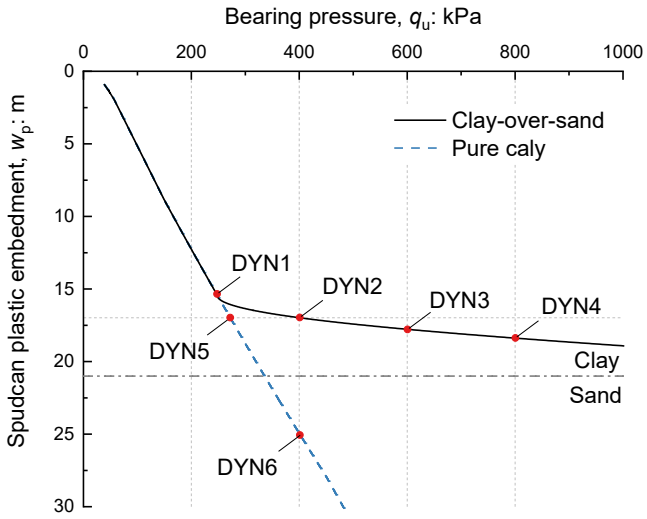

Figure 5. Spudcan vertical load-penetration curve

Figure 6 shows the surface elevation of a NewWave, characterised by a crest elevation of 8 m. Notably, an asymmetry in wave heights is observed between the windward and leeward legs due to spatial variations among the legs (with the symmetric NewWave directly under the HRP).

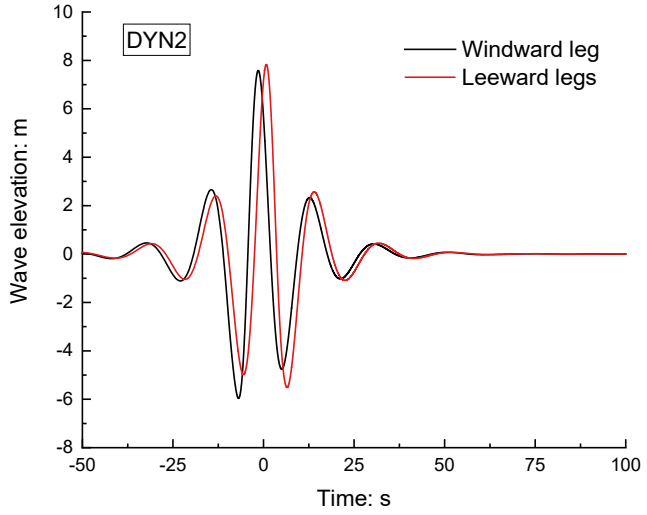

Figure 6. NewWave elevations at jack-up leg locations

Figure 7 shows the horizontal displacement of the hull in response to NewWave loading with varying amplitudes of 8, 12, and 15 m. While only the horizontal hull displacement is depicted, other indicators of structural response can also be obtained. It is evident that the amplitude of displacement increases with higher wave amplitudes. Subsequent to the passage of the NewWave, observable vibrations occur in the jack-up structure, resonating with its natural mode. For the specific macro-element model employed in this paper, the natural period of the jack-up is 8.0 s. When examining the hull offsets, it is observed that negligible deviations of -0.01 m are noticeable for wave amplitudes of 8 m and 12 m. However, a substantial permanent offset of 0.43 m is evident when the wave amplitude is 15 m. This notable permanent offset arises due to the expansion of the yield surface induced by the loading, subsequently resulting in plastic displacement within the macro-element model footings. Consequently, the entire foundation undergoes a shift, leading to a lasting offset in hull displacement. Furthermore, the natural period of the system experiences elongation due to the degradation of foundation stiffness throughout the plastic behaviour.

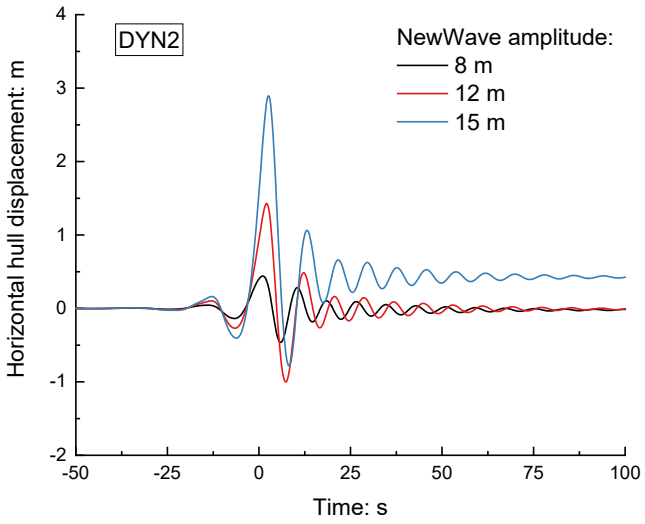

Figure 7. Horizontal hull displacements of the jack-up

EFFECT OF THE UNDERLYING SAND

The dynamic analysis results concerning the spudcan embedment at varying depths in close proximity to the underlying sand layer are shown in Figure 8, with NewWave crest elevation of 8 m. The natural periods of the jack-up structure are recorded as 8.6, 8.0, 7.7, and 7.4 s, respectively. Notably, these periods exhibit an ascending trend as the spudcan approaches the underlying sand stratum. This observed pattern aligns with expectations, stemming from the increase in foundation stiffness. Consequently, the overall system stiffness experiences a corresponding increase. This phenomenon is attributed to the heightened contribution of the strong underlying sand layer.

Furthermore, the extracted peak horizontal displacements of the hull are presented in the inset of Figure 8. It is noteworthy that these displacements undergo a reduction as the spudcan's proximity to the clay-sand interface diminishes. These findings substantiate the potential for practitioners to strategically position the spudcan in close proximity to the strong underlying sand layer (provided that the necessary preload criterion can be met). This positioning aims to effectively reduce the extent of jack-up displacement during storm events.

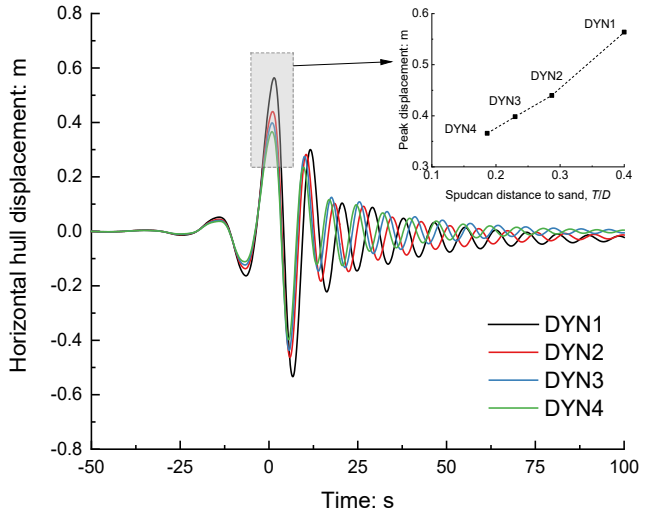

Figure 8. Horizontal hull displacements at four spudcan embedments

COMPARISON WITH PURE CLAY RESULTS

The comparative analysis employs the macro-element model established by Zhang et al. (2014)[10] for buried spudcans in soft clay featuring soil backflow. This model is juxtaposed against the macro-element model designed for scenarios where clay overlies sand. The results of this analysis are shown in both Figure 9 and

Figure 10, considering the two scenarios of identical embedment depths and matching preload magnitudes, respectively.

In Figure 9, focusing on the identical embedment depth, a pronounced reduction in hull displacement amplitude is observed in the clay-over-sand condition. Notably, the natural period also experiences a decline, decreasing from 9.2 s in the case of pure clay to 8.0 s for the layered soil scenario. A comparative examination reveals a more substantial permanent hull offset of -0.08 m for the jack-up structure in pure clay, in contrast to the -0.01 m offset observed in clay-over-sand. This augmented permanent offset in pure clay is attributed to foundation yielding due to a smaller yield surface stemming from the relatively lower preload level.

Shifting the focus to Figure 10, where an identical preload magnitude is considered, a slight reduction in displacement amplitude is evident under the clay-over-sand configuration. While a similar dynamic response with a natural period of 8.4 s is discerned in the scenario involving pure clay, achieving this preload level of 400 kPa necessitates a 47% deeper penetration depth. This requirement points towards an elongated jack-up leg length.

These comparative analyses underscore the critical importance of a precise assessment of spudcan stiffness, along with the subsequent determination of the jack-up's natural period. It is imperative to employ a suitable macro-element model tailored to the characteristics of layered soil conditions to ensure accurate evaluations.

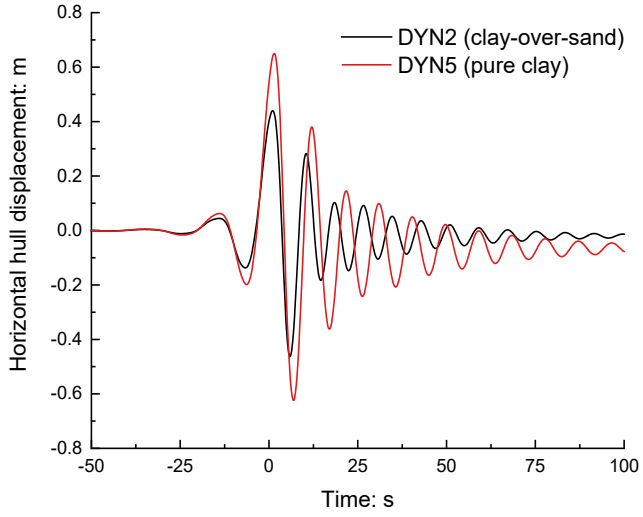

Figure 9. Horizontal hull displacements in pure clay and clay-over-sand (identical embedment depth)

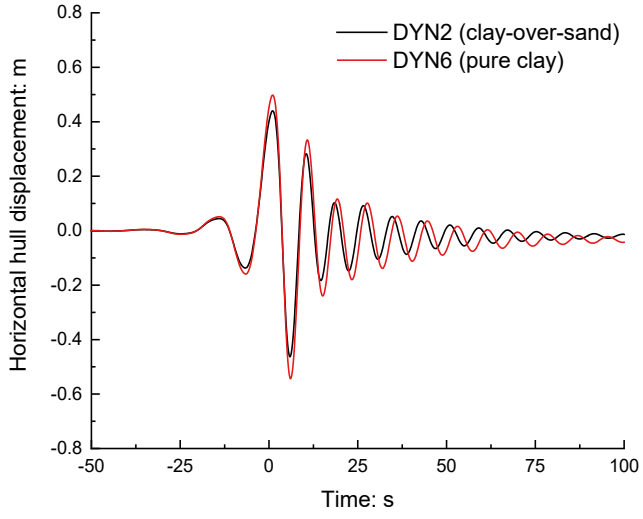

Figure 10. Horizontal hull displacements in pure clay and clay-over-sand (identical preload magnitude)

CONCLUSIONS

This study has provided an investigation into the dynamic behaviour of jack-up units installed in clay overlying sand when subjected to storm loading. Through the utilisation of a macro-element model, the interaction between spudcan footings and the layered soil has been effectively characterised. The adoption of the NewWave theory has further enabled the accurate representation of wave loading on the structure.

The dynamic time-domain simulations have unveiled the significant influence of the underlying sand layer on the overall system response. The increased foundation stiffness due to the presence of the sand layer leads to a concomitant increase in system stiffness and reduction in the natural period. Furthermore, the mitigated hull displacement and permanent offset following wave passage demonstrate the strategic benefits of situating spudcans near the underlying strong sand layer.

By contrasting scenarios involving jack-ups in pure clay, this study accentuates the necessity of adopting a tailored foundation modelling for layered soil conditions. The substantial influence of footing response on system behaviour in layered soil scenarios is evident. Consequently, practitioners and researchers are urged to embrace appropriate foundation modelling to accurately capture the complexities inherent in layered soil configurations.

REFERENCES

[1] Schotman, G.J.M. The effects of displacements on the stability of jack-up spudcan foundations. In: Proc. 21st Offshore Technology Conference, Offshore Technology Conference, Houston, TX, USA, 1989.

[2] Dean, E.T.R., James, R.G., Schofield, A.N., Tsukamoto, Y. Theoretical modelling of spudcan behaviour under combined load, Soils and Foundations. 1997a: 37 (2): 1-15.

[3] Dean, E.T.R., James, R.G., Schofield, A.N., Tsukamoto, Y. Numerical modelling of three-leg jackup behaviour subject to horizontal load, Soils and Foundations. 1997b: 37 (2): 17-26.

[4] van Langen, H., Wong, P.C., Dean, E.T.R. Formulation and validation of a theoretical model for jack-up foundation load-displacement assessment, Marine Structures. 1999: 12 (4): 215-230.

[5] Martin, C.M., Houlsby, G.T. Combined loading of spudcan foundations on clay: numerical modelling, Géotechnique. 2001: 51 (8): 687-699.

[6] Cassidy, M.J., Byrne, B.W., Houlsby, G.T. Modelling the behaviour of circular footings under combined loading on loose carbonate sand, Géotechnique. 2002: 52 (10): 705-712.

[7] Houlsby, G.T., Cassidy, M.J. A plasticity model for the behaviour of footings on sand under combined loading, Géotechnique. 2002: 52 (2): 117-129.

[8] Bienen, B., Byrne, B.W., Houlsby, G.T., Cassidy, M.J. Investigating six-degree-of-freedom loading of shallow foundations on sand, Géotechnique. 2006: 56 (6): 367-379.

[9] Vlahos, G., Cassidy, M.J., Byrne, B.W. The behaviour of spudcan footings on clay subjected to combined cyclic loading, Applied Ocean Research. 2006: 28 (3): 209-221.

[10] Zhang, Y., Cassidy, M.J., Bienen, B. A plasticity model for spudcan foundations in soft clay, Canadian Geotechnical Journal. 2014: 51 (6): 629-646.

[11] Cheng, N., Cassidy, M.J. Development of a force–resultant model for spudcan footings on loose sand under combined loads, Canadian Geotechnical Journal. 2016: 53 (12): 2014-2029.

[12] Wang, Y., Cassidy, M.J., Bienen, B. A macro-element model for predicting the combined load behaviour of spudcan foundations in clay overlying sand, Géotechnique. 2023: 73 (4): 281-293.

[13] Wang, Y., Cassidy, M.J., Bienen, B. Numerical pushover analysis of jack-up units in soft clay overlying sand, Ocean Engineering. 2022: 258: 111762.

[14] Bienen, B., Cassidy, M.J. Advances in the three-dimensional fluid–structure–soil interaction analysis of offshore jack-up structures, Marine Structures. 2006: 19 (2–3): 110-140.

[15] Tromans, P.S., Anaturk, A.R., Hagemeijer, P. A new model for the kinematics of large ocean waves - application as a design wave. In: Proc. 1st International Offshore and Polar Engineering Conference, International Society of Offshore and Polar Engineers, ISOPE, 1991. p 64-71.

[16] Taylor, P.H., Jonathan, P., Harland, L.A. Time domain simulation of jack-up dynamics with the extremes of a gaussian process, Journal of Vibration and Acoustics. 1997: 119 (4): 624-628.

[17] Cassidy, M.J., Taylor, R.E., Houlsby, G.T. Analysis of jack-up units using a Constrained NewWave methodology, Applied Ocean Research. 2001: 23 (4): 221-234.

[18] Houlsby, G.T., Martin, C.M. Undrained bearing capacity factors for conical footings on clay, Géotechnique. 2003: 53 (5): 513-520.

[19] Hossain, M.S., Randolph, M.F. New mechanism-based design approach for spudcan foundations on single layer clay, Journal of Geotechnical and Geoenvironmental Engineering. 2009: 135 (9): 1264-1274.
[20] Wang, Y., Cassidy, M.J., Bienen, B. Evaluating the penetration resistance of spudcan foundations in clay overlying sand, International Journal of Offshore and Polar Engineering. 2021: 31 (02): 243-253.
[21] Zhang, Y., Bienen, B., Cassidy, M.J. Jack-up push-over analyses featuring a new force resultant model for spudcans in soft clay, Ocean Engineering. 2014: 81: 139-149.
[22] Wang, Y., Cassidy, M.J., Bienen, B. Numerical investigation of bearing capacity of spudcan foundations in clay overlying sand under combined loading, Journal of Geotechnical and Geoenvironmental Engineering. 2020: 146 (11): 04020117.
[23] Cassidy, M.J., Houlsby, G.T., Hoyle, M., Marcom, M.R. Determining appropriate stiffness levels for spudcan foundations using jack-up case records. In: Proc. 21st International Conference on Offshore Mechanics and Arctic Engineering, 2002. p 307-318.
[24] Doherty, J.P., Deeks, A.J. Elastic response of circular footings embedded in a non-homogeneous half-space, Géotechnique. 2003: 53 (8): 703-714.
[25] Zhang, Y., Cassidy, M.J., Bienen, B. Elastic stiffness coefficients for an embedded spudcan in clay, Computers and Geotechnics. 2012: 42: 89-97.
[26] Wang, Y., Cassidy, M.J., Bienen, B. Elastic stiffness of circular footings on clay overlying sand under general loading, Géotechnique Letters. 2020: 10 (4): 498-509.